
LLMs are Bayesian, In Expectation, Not in Realization

Leon Chlon^{1,2} Zein Khamis¹ Maggie Chlon¹ Mahdi El Zein¹ MarcAntonio Awada¹

Abstract

Exchangeability-based martingale diagnostics have been used to question Bayesian explanations of transformer in-context learning. We show these violations are compatible with Bayesian/MDL behavior once we account for a basic architectural fact: positional encodings break exchangeability, so the relevant baseline is performance *in expectation over orderings of an exchangeable multiset*, not for every ordering. In a Bernoulli microscope (under explicit regularity assumptions), we bound the permutation-induced dispersion detected by martingale diagnostics (Theorem 3.4) while proving near-optimal expected MDL/compression over permutations (Theorem 3.6). Empirically, black-box next-token logprobs from an Azure OpenAI deployment exhibit nonzero gaps that decay with context length (mean 0.74 at $n=10$ to 0.26 at $n=50$; 95% CIs) and permutation averaging reduces order-induced standard deviation with a $k^{-1/2}$ trend (Figure 2). Controlled from-scratch training ablations varying only the positional encoding show within-prefix order variance collapsing to $\approx 10^{-16}$ with no PE but remaining 10^{-8} – 10^{-6} under standard PE schemes (Table 2); robustness checks extend beyond Bernoulli to categorical sequences, synthetic ICL tasks, and evidence-grounded QA with permuted exchangeable evidence chunks.

Our starting point is architectural: positional encodings break permutation invariance, so the right baseline is not Bayes-optimality *for every ordering* but Bayes/MDL optimality *in expectation over random orderings of the observed multiset*. We make this precise in a controlled Bernoulli model and quantify both the unavoidable gap and a practical mitigation via permutation averaging.

Contributions. We focus the main paper on three claims that can be checked quickly against specific evidence:

- **Nonzero order-induced gaps from position-awareness.** Under regularity assumptions, the induced permutation sensitivity admits an explicit finite- n upper bound with interpretable constants (Theorem 3.4).
- **Near-optimal compression in expectation.** Position-aware predictors achieve near-optimal MDL *in expectation over random orderings of the same multiset* (Theorem 3.6); we additionally give an informal mechanistic sketch connecting permutation-averaged behavior to pseudo-count Bayesian updates (Appendix A.4).
- **Permutation averaging as a practical fix.** Averaging over k random orderings provides a Monte Carlo estimate of permutation-averaged prediction, reducing the *standard deviation* of order-induced variability $\propto k^{-1/2}$ (equivalently, variance $\propto k^{-1}$) and yielding an explicit $O((kn)^{-1/2})$ upper bound under our assumptions when combined with Theorem 3.4 (Proposition 3.8; Figures 1–2).

1. Introduction

Large language models exhibit strong in-context learning behavior, and a popular explanation is that transformers approximate Bayesian inference over latent task variables (Xie et al., 2022; Bai et al., 2023). Yet recent empirical tests show systematic martingale/exchangeability violations relative to Bayesian posterior prediction on exchangeable data (Falck et al., 2024).

¹Hassana Labs ²University of Oxford. Correspondence to: Leon Chlon <leo@hassana.io>.

Key results and where they appear.

- **Claim 1 (order-induced gaps):** Theorem 3.4; Exp. 2/3/5 with black-box logprobs (Sec. 4; Figure 1; Table 1); PE ablation (Table 2).
- **Claim 2 (expected MDL near-optimality):** Theorem 3.6; controlled MDL experiment (Exp. 8; Table 2).
- **Claim 3 (permutation averaging):** Proposition 3.8; synthetic ICL k -sweep (Exp. 10; Figure 2) and evidence-grounded QA mixtures (Exp. 14; Appendix B.6).

We defer proofs, additional experiments, and extended discussions to the appendix.

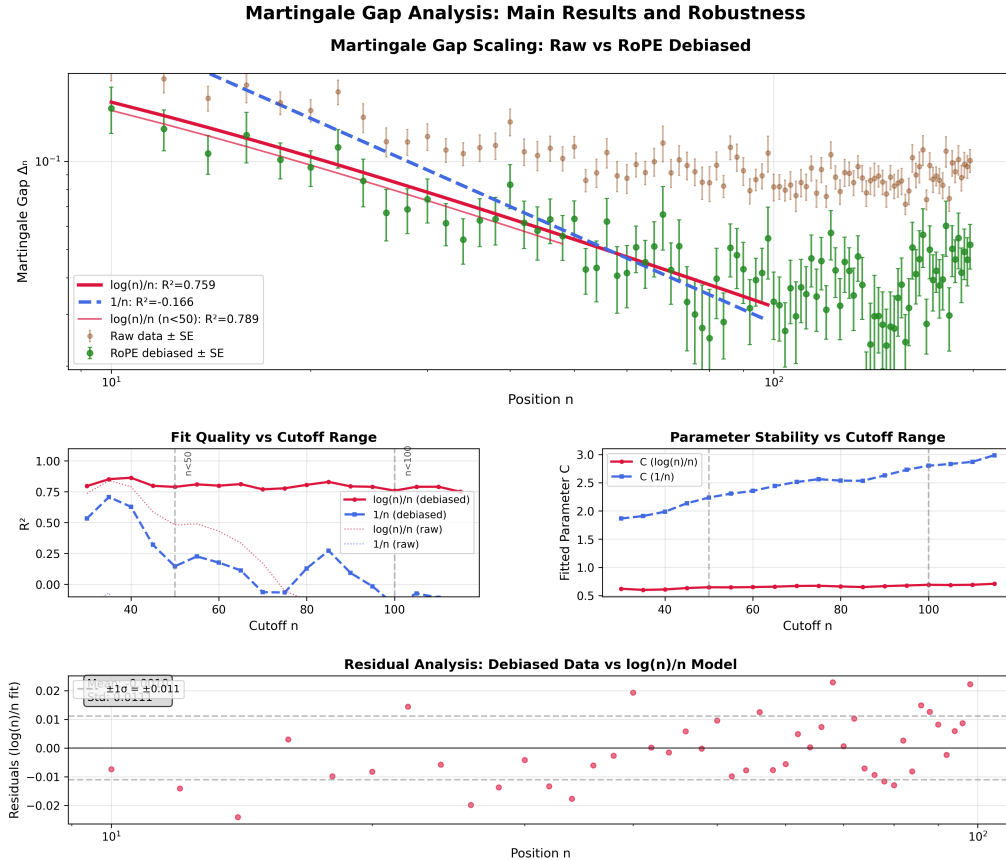


Figure 1. Martingale gaps and periodic components. Proxy gaps $\hat{\Delta}_n$ decrease with n and exhibit periodic structure; a debiasing step removes the period-64 component while preserving the slower trend (Sec. 4).

2. Setup and Related Work

Bayesian ICL and martingale tests. Bayesian posterior prediction on exchangeable data is permutation-invariant and satisfies martingale-style constraints. Recent tests report systematic martingale/exchangeability violations in pre-trained transformers (Falck et al., 2024), which can be read as evidence against a literal “Bayesian for every ordering” interpretation.

Positional encodings break exchangeability. Transformers require positional information (absolute/sinusoidal, RoPE, ALiBi, etc.), which breaks permutation invariance by design. This motivates an *average-case* notion: performance in expectation over random orderings of the observed multiset. Our theory makes this explicit in a Bernoulli sequence model, where $S_n = \sum_{i=1}^n x_i$ is sufficient.

When a permutation baseline is normative (and when it is not). Our permutation expectations are intended for settings where the observed input is exchangeable as a *multiset* but must be linearized for a sequence model: few-shot demonstrations, retrieved evidence chunks, or unordered

records. Next-token training minimizes expected negative log-likelihood under the training distribution over sequences; when sequences arise by choosing an ordering π of a fixed multiset, this objective is an expectation over π (i.e., an expected conditional description length over orderings). In the absence of a canonical ordering, the maximum-entropy choice is $\pi \sim \text{Unif}(\mathfrak{S}_n)$; more generally, our Monte Carlo averaging statements hold for any order distribution by sampling i.i.d. orderings from that distribution. We do *not* claim uniform permutations are a baseline for general language modeling where word order carries semantics. In Exp. 14 (Factuality Slice) we check the nuisance-order viewpoint in evidence-grounded QA, where the same set of evidence chunks is presented in different orders: uniform permutation mixtures yield consistent Jensen gains and are near-optimal among convex mixtures (Appendix B.6).

Two permutation baselines (global vs. within-prefix). For horizon n , the Bernoulli sufficient statistic is the final count S_n , and “random orderings of the same multiset” simply means averaging over all $n!$ permutations of the length- n multiset. For online predictions at time $t \ll n$, however, a

global permutation that preserves S_n can still change the prefix count S_t ; a Bayesian predictor is allowed to change with S_t . Therefore, when we empirically test order sensitivity at a fixed t , we condition on (t, S_t) and permute only within the prefix. We use the term *global permutations* for the theorem-aligned Δ_n (Theorem 3.4) and *within-prefix permutations* for the stronger sufficient-statistic control in Exp. 3.

MDL/compression as a unifying lens. We use description length (MDL) (Grünwald, 2007) to connect predictive performance to an information-theoretic optimum: a predictor can be near-optimal in expected compression while still exhibiting order-dependent deviations on any fixed realization.

3. Theoretical Analysis

We now present our main theoretical results, establishing how positional encodings create an inherent tension between architectural expressiveness and statistical exchangeability.

3.1. Problem Formulation

Consider binary sequences $X = (x_1, \dots, x_n)$ with $x_i \in \{0, 1\}$ drawn i.i.d. from Bernoulli(p), where $p \in [0, 1]$ is unknown. We analyze transformer predictions under two configurations:

Definition 3.1 (Position-Aware Transformer). A transformer \mathcal{T}_θ with parameters θ and positional encoding $\text{PE} : \mathbb{N} \rightarrow \mathbb{R}^d$ computes:

$$P_{\mathcal{T}}(x_{t+1} = 1 | x_{1:t}) = \sigma(f_\theta(\text{Embed}(x_{1:t}) + \text{PE}(1 : t))) \quad (1)$$

where σ is the sigmoid function and f_θ represents the full transformer computation.

Definition 3.2 (Position-Agnostic Transformer). The same architecture without positional information:

$$P_{\mathcal{T}^\emptyset}(x_{t+1} = 1 | x_{1:t}) = \sigma(f_\theta(\text{Embed}(x_{1:t}))) \quad (2)$$

The distinction between these configurations is crucial: position-agnostic transformers can only access information through the multiset of tokens, while position-aware transformers additionally leverage ordering information.

3.2. Martingale-Property Baseline and Order Sensitivity

Following the martingale-property viewpoint of Falck et al. (2024), an exchangeable Bayesian learning system induces predictive distributions that (i) are invariant to the order in which i.i.d. samples are revealed and (ii) evolve coherently as a martingale with respect to the filtration generated by revealed samples. We make this explicit in our Bernoulli sandbox.

Lemma 3.3 (Exchangeable Bayes Baseline Across Orderings). *Let $(X_i)_{i \geq 1}$ be exchangeable, and for any ordering π define the online filtration $\mathcal{F}_t^\pi := \sigma(X_{\pi(1)}, \dots, X_{\pi(t)})$. In the Bernoulli model with latent parameter p (and any prior), the Bayesian posterior predictive mean*

$$m_t^\pi := \mathbb{P}(X_{\pi(t+1)} = 1 | \mathcal{F}_t^\pi) = \mathbb{E}[p | \mathcal{F}_t^\pi] \quad (3)$$

is (a) order-invariant—it is a function only of the multiset $\{X_{\pi(1)}, \dots, X_{\pi(t)}\}$ (equivalently of the count $S_t = \sum_{i=1}^t X_{\pi(i)}$)—and (b) a martingale with respect to $(\mathcal{F}_t^\pi)_{t \geq 0}$, i.e. $\mathbb{E}[m_{t+1}^\pi | \mathcal{F}_t^\pi] = m_t^\pi$.

Position-aware transformers violate the order-invariance premise by construction, so exchangeability-based martingale diagnostics can register nonzero gaps even when the model remains near-optimal in *expected* MDL/compression over orderings. We now quantify the induced order sensitivity.

Theorem 3.4 (Quantified Order-Induced Gap (Upper Bound)). *Fix a length- n Bernoulli multiset with sufficient statistic $S_n = \sum_{i=1}^n x_i$, and draw a uniform random permutation $\pi \sim \text{Unif}(\mathfrak{S}_n)$ (i.e., a uniform random ordering of the same multiset). Assume the model’s next-token logit depends on the ordering only through the positional summary*

$$u_\pi := \frac{1}{n} \sum_{i=1}^n x_{\pi(i)} \text{PE}(i) \in \mathbb{R}^d \quad (4)$$

and that the logit map is L_f -Lipschitz in u_π (with other features fixed by S_n).¹ Define the positional-encoding variance at length n as

$$\sigma_{PE}^2 := \frac{1}{n} \sum_{i=1}^n \left\| \text{PE}(i) - \frac{1}{n} \sum_{j=1}^n \text{PE}(j) \right\|^2. \quad (5)$$

Let $P_\pi(y) := P_{\mathcal{T}}(y | X_{\pi(1:n)})$ and define $s(\pi) := \mathbb{E}_{Y \sim \text{Bernoulli}(p)}[\log P_\pi(Y)]$. Then the order-induced standard deviation

$$\Delta_n := \sqrt{\text{Var}_\pi[s(\pi) | X_{1:n}]} \quad (6)$$

is bounded as

$$\begin{aligned} \Delta_n &\leq L_f \sigma_{PE} \sqrt{\frac{S_n(n - S_n)}{n^2(n - 1)}} \\ &\leq \frac{L_f \sigma_{PE}}{2\sqrt{n - 1}}. \end{aligned} \quad (7)$$

The proof (Appendix) makes the permutation distribution explicit and bounds the induced variation by analyzing random assignments of the S_n ones to positions.

¹This abstraction isolates the simplest position–token interaction: a correlation between token identity and positional encodings. It is exact for linear readouts on pooled position–token features, and serves as a conservative bound for more complex architectures.

How the constants relate to transformers (and how to estimate them). The bound separates (i) *positional geometry* through σ_{PE} , which is determined entirely by the chosen positional encoding and the context length, and (ii) an *effective position sensitivity* L_f , which summarizes how strongly a model’s output logit changes as the position–token summary u_π changes. For white-box models, L_f can be upper-bounded (or locally estimated) via gradient norms of the relevant logit with respect to u_π , and σ_{PE} can be computed directly from the encoding. For black-box LLM deployments we do not claim a direct mapping from L_f to parameter norms; instead, we test the theory’s qualitative implications (order-induced dispersion, its decay with n , and $k^{-1/2}$ variance reduction from averaging) directly in controlled and real transformer settings (Sec. 4, Exp. 14).

3.3. Information-Theoretic Optimality

Despite violating martingale properties, we show that transformers achieve near-optimal compression rates:

Definition 3.5 (Empirical MDL). For model M and data $X_{1:n}$, the empirical Minimum Description Length is:

$$\text{MDL}_n(M, X_{1:n}) = L(M) + \sum_{t=1}^n [-\log P_M(X_t | X_{1:t-1})] \quad (8)$$

where $L(M)$ is the description length of model M .

Theorem 3.6 (MDL Optimality of Position-Aware Transformers). A transformer \mathcal{T}_{θ^*} trained on sequences from Bernoulli(p) achieves expected MDL optimality:

$$\mathbb{E}_{X,\pi}[\text{MDL}_n(\mathcal{T}_{\theta^*}, X_{\pi(1:n)})] = nH(p) + O(\sqrt{n \log n}) \quad (9)$$

where the expectation is over data X and uniform random permutations π .

The proof shows that transformers learn to compress based on sufficient statistics, achieving the information-theoretic limit up to lower-order terms. Crucially, this optimality holds in expectation over orderings, not for any specific ordering.

3.4. Implicit Bayesian Representations (Mechanistic Sketch)

Remark 3.7 (Implicit pseudo-count behavior (informal)). In the Bernoulli model, a Beta prior with pseudo-counts (α_0, β_0) yields the posterior predictive mean

$$\mathbb{P}(X_{t+1} = 1 | X_{1:t}) = \mathbb{E}[p | X_{1:t}] = \frac{\alpha_0 + S_t}{\alpha_0 + \beta_0 + t}. \quad (10)$$

Although a position-aware transformer can be order-sensitive on any fixed realization, our controlled results show that its *permutation-averaged* compression is close to

count-based baselines (Sec. 4, Exp. 8). Appendix A.4 gives a mechanistic sketch for how attention can approximate counts and how an MLP can map them to pseudo-count-like predictions; we treat this as an interpretation rather than a theorem-level guarantee.

3.5. Putting the Pieces Together

Theorem 3.4 quantifies unavoidable order-induced variability when predictions correlate with positional encodings, while Theorem 3.6 shows that a position-aware predictor can still be near-optimal in *expected* compression over random orderings. Together, these results support the paper’s central message: a transformer can look “Bayesian/MDL-like in expectation” while failing exchangeability-based martingale tests on individual orderings, because positional information breaks the invariances those tests assume.

3.6. Practical Implications

Our theoretical analysis yields concrete algorithms for uncertainty quantification:

Proposition 3.8 (Permutation Averaging: Monte Carlo Variance Reduction). Fix a multiset $X_{1:n}$ and draw i.i.d. permutations $\pi_1, \dots, \pi_k \sim \text{Unif}(\mathfrak{S}_n)$. For a position-aware transformer \mathcal{T} , define the permutation-averaged predictor estimated from k samples as

$$\bar{P}_k(x_{n+1} | X_{1:n}) = \frac{1}{k} \sum_{i=1}^k P_{\mathcal{T}}(x_{n+1} | X_{\pi_i(1:n)}) \quad (11)$$

Let $Z_\pi := P_{\mathcal{T}}(x_{n+1} | X_{\pi(1:n)})$, so $\bar{P}_k(x_{n+1} | X_{1:n}) = \frac{1}{k} \sum_{i=1}^k Z_{\pi_i}$. Then, for any fixed label x_{n+1} ,

$$\text{Var}[\bar{P}_k(x_{n+1} | X_{1:n}) | X_{1:n}] = \frac{1}{k} \text{Var}_\pi[Z_\pi | X_{1:n}], \quad (12)$$

so the corresponding standard deviation scales as $k^{-1/2}$. Moreover, if we instead average the expected log score statistic

$$s(\pi) := \mathbb{E}_{Y \sim \text{Bernoulli}(p)}[\log P_{\mathcal{T}}(Y | X_{\pi(1:n)})], \quad (13)$$

then

$$\text{Std}\left[\frac{1}{k} \sum_{i=1}^k s(\pi_i) \middle| X_{1:n}\right] = \frac{1}{\sqrt{k}} \Delta_n \leq \frac{L_f \sigma_{PE}}{2\sqrt{k(n-1)}} \quad (14)$$

by Theorem 3.4.

Additional practical options include conditioning on sufficient statistics (when available) and position-agnostic fine-tuning; here we focus on permutation averaging.

4. Empirical Validation

We validate the observable implications of our theory using (i) black-box next-token log probabilities from Azure OpenAI Chat Completions deployments, (ii) controlled from-scratch training ablations where we vary only the positional encoding scheme, and (iii) an evidence-grounded QA setting where evidence is exchangeable but its presentation order varies (Exp. 14). The suite measures: (i) how the proxy martingale gap varies with context length in a Bernoulli sandbox, (ii) how that proxy relates to the theorem-aligned permutation gap Δ_n (Theorem 3.4) in a controlled Bernoulli setting, (iii) order sensitivity under within-prefix permutations holding sufficient statistics fixed, and (iv) order-induced variability and Monte Carlo variance reduction from permutation averaging on procedurally generated in-context learning (ICL) tasks, categorical sequences, and exchangeable evidence chunks. Black-box runs use `temperature=0`, `max_tokens=1`, and `top_logprobs=20` to extract logprobs for a fixed small label set (binary: 0/1; categorical: A/B/C; ICL tasks: A/B).

4.1. Black-Box Setup

We use a fixed “headered” prompt format that explicitly enumerates the allowed labels (e.g., “Respond with exactly one of {0, 1}”). A robustness sweep (Exp. 4) shows that this avoids logprob extraction failures: across 18 prompt variants, headered prompts have a 0.0 missing rate while headerless prompts fail almost always (mean missing ≈ 0.996). Unless otherwise stated, all reported results use the headered format and have 0.0 missing rate.

For binary Bernoulli experiments, we generate balanced sequences (even n with $n/2$ zeros and $n/2$ ones) and measure the proxy gap

$$\hat{\Delta}_n = \mathbb{E}_{\text{seq}} [|\log P_{\mathcal{T}}(x_n|x_{1:n-1}) - \log P_{\mathcal{T}}(x_n|x_{1:n-2})|] \quad (15)$$

which corresponds to the paper’s original estimand. We additionally estimate the theorem-aligned permutation gap Δ_n in a controlled Bernoulli setting by (i) extracting logprobs for both outcomes to compute the expected log score under $Y \sim \text{Bernoulli}(p)$ for each ordering and (ii) measuring its variability across uniform random permutations of the same length- n multiset.

4.2. Results

Results at a glance. In Bernoulli sequences at $p = \frac{1}{2}$, the mean proxy gap decreases from 0.74 at $n = 10$ to 0.26 at $n = 50$ (Exp. 2). In a controlled Bernoulli setting, the proxy gap tracks the theorem-aligned permutation gap Δ_n from Theorem 3.4 (Exp. 2). Under within-prefix sufficient-statistic controls, order still matters ($\text{Var}[p_1] = 1.0 \times 10^{-2}$ at $t = 20$ and 2.4×10^{-3} at $t = 200$; Exp. 3), and

in controlled from-scratch ablations this sensitivity collapses under no-PE by roughly 8–10 orders of magnitude ($\text{Var}[p] \approx 10^{-16}$ vs 10^{-8} – 10^{-6} ; Table 2). On procedurally generated ICL tasks, demo order induces variance (mean $\text{Var}[p_A] = 0.0178$ threshold and 0.0370 linear2d) and permutation averaging reduces the standard deviation of the averaged prediction with a $k^{-1/2}$ trend (Exp. 10; Fig. 2). Beyond Bernoulli, a 3-symbol categorical analogue shows nonzero gaps with the same qualitative decay (1.23 at $n = 12$ to 0.30 at $n = 120$; Exp. 13). Finally, in evidence-grounded QA where evidence chunks are exchangeable, permuting the same evidence set changes model probabilities and uniform permutation mixtures yield positive Jensen gains (0.104 and 0.0098 nats/token in two open models) while being essentially optimal among convex mixtures (Exp. 14; Appendix B.6). In the same controlled setting, expected compression regret vs KT is ≈ 0.002 bits/token at $n = 200$ (Exp. 8; Table 2). Where possible we report 95% bootstrap confidence intervals (CIs) by resampling independent units (sequences, tasks, or permutations).

4.2.1. BERNOULLI GAP VS. CONTEXT LENGTH

We first test the core empirical prediction that position-awareness produces nonzero gaps that decay with context length. Figure 1 summarizes the gap-vs- n trend and periodic components. In our black-box Bernoulli run at $p = \frac{1}{2}$ with $n \in \{10, 12, \dots, 50\}$ and 50 balanced sequences per n , the mean proxy gap decreases from 0.74 (95% CI [0.40, 1.17]) at $n = 10$ to 0.26 (95% CI [0.19, 0.33]) at $n = 50$ (0.0 missing rate). A held-out scaling comparison on these points slightly prefers $\log n/n$ over $1/n$, but the evidence is necessarily modest at this short n range.

4.2.2. ESTIMAND CHECK: PROXY GAP VS. THEOREM-ALIGNED PERMUTATION GAP

Theorem 3.4 is stated in terms of a permutation-induced gap Δ_n defined via expected log scores under $Y \sim \text{Bernoulli}(p)$. In a controlled Bernoulli setting (known p), we estimate this quantity by extracting logprobs for both symbols, computing the expected log score for each ordering, and then measuring its variability across uniform random permutations of the same length- n multiset. This is distinct from Exp. 3 below, which conditions on (t, S_t) and permutes only within the prefix as a stronger sufficient-statistic control. We report both the proxy gap and the theorem-aligned estimate to make the estimand relationship explicit.

4.2.3. WITHIN-PREFIX PERMUTATIONS (SUFFICIENT-STATISTIC CONTROL)

Balancing the final count S_n does not control prefix-dependent conditioning. We therefore fix a prefix length

Threat to validity	Targeted check	Outcome
Estimand mismatch	Exp. 2 (proxy vs theorem)	Proxy gap tracks the theorem-aligned permutation gap Δ_n in a controlled Bernoulli setting.
Prefix-statistic control	Exp. 3 (within-prefix perms)	Holding S_t fixed and permuting within the prefix yields nontrivial order variance ($\text{Var}[p_1] \approx 1.0 \times 10^{-2}$ at $t = 20$; $\approx 2.4 \times 10^{-3}$ at $t = 200$).
Attribution to positional information	Controlled PE ablation (Exp. 3)	In trained-from-scratch models, no-PE yields essentially zero within-prefix order variance ($\approx 10^{-16}$), while PE variants yield nonzero variance (10^{-8} – 10^{-6}).
Prompt/token artifacts	Exp. 4 (robustness)	Headered prompts: 0.0 missing across 18 variants; headerless prompts: near-total extraction failure.
Position-index artifacts	Exp. 5 (phase shift)	Prepending neutral tokens changes the measured gaps (max change ≈ 0.2 over tested offsets), consistent with absolute-position effects.
External validity	Exp. 10/11, Exp. 13, Exp. 14	Order-induced variability appears on procedurally generated ICL tasks, categorical sequences, and evidence-grounded QA under exchangeable evidence permutations; averaging over k permutations reduces standard deviation $\propto k^{-1/2}$ (variance $\propto k^{-1}$; Fig. 2).

Table 1. **Targeted validation suite.** Each experiment addresses a concrete threat to validity (estimand mismatch, insufficient-statistic controls, prompt artifacts, position-index artifacts, attribution to positional information, and external validity). Full protocols and raw outputs are in the appendix.

t and count S_t , and permute only within the prefix. Even under this control, the model’s next-token probability varies across orderings: at $t = 20$, $\text{Var}[p_1] = 1.02 \times 10^{-2}$ (95% CI $[0.53, 1.69] \times 10^{-2}$), while at $t = 200$, $\text{Var}[p_1] = 2.44 \times 10^{-3}$ (95% CI $[1.95, 2.96] \times 10^{-3}$) (200 within-prefix permutations per t ; 0.0 missing rate). This isolates order/position dependence while holding the prefix sufficient statistic fixed.

Controlled ablation (from-scratch training). To isolate positional information as the source of order sensitivity, we train small transformers on i.i.d. Bernoulli sequences while varying only the positional encoding scheme (none, learned absolute, sinusoidal, RoPE, ALiBi). Evaluating Exp. 3 on these models shows a sharp separation: the no-PE model has essentially zero within-prefix order variance (e.g., $\text{Var}[p] \approx 3.7 \times 10^{-16}$ at $t = 20$), while PE variants have nonzero variance (10^{-8} – 10^{-6}), an ≈ 8 – 10 order-of-magnitude increase. This pins the order sensitivity (and hence martingale/exchangeability violations) on positional information in a controlled setting, motivating expected performance under random orderings (global permutations) as the relevant baseline for Bayesian/MDL behavior. Table 2 summarizes these ablations and the corresponding MDL results.

4.2.4. PERMUTATION AVERAGING

We next test the practical implication that averaging over random demo orderings reduces order-induced variability. On procedurally generated ICL tasks (200 tasks, 8 demonstrations per task, 20 random orders per task), demo order induces measurable uncertainty even when the underlying task is unchanged: the mean variance of p_A across orders is 0.0178 (95% CI $[0.0115, 0.0250]$) for threshold and 0.0370

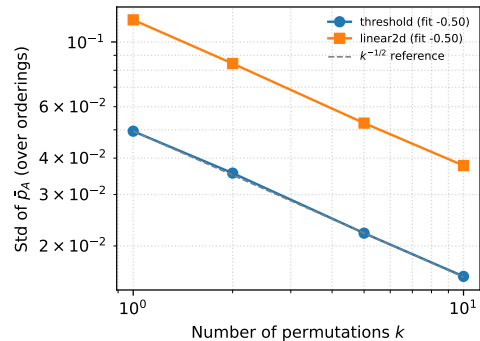


Figure 2. **Permutation averaging reduces order-induced standard deviation on ICL tasks.** We generate procedurally defined few-shot classification tasks (threshold and linear2d), hold the demonstration set fixed, and vary only the demo order (200 tasks; 20 random orders per task). For each task we estimate $\text{Std}(\bar{p}_A)$ under k independent random orderings (resampling permutations with replacement); the resulting decay is consistent with $k^{-1/2}$.

(95% CI $[0.0295, 0.0453]$) for linear2d. Averaging over k independent random demo orderings reduces the standard deviation of \bar{p}_A with a $k^{-1/2}$ trend: fitted slopes are -0.498 (95% CI $[-0.512, -0.482]$) and -0.499 (95% CI $[-0.508, -0.490]$) respectively (bootstrap over tasks). We also compare permutation averaging to template averaging (Exp. 11): on these tasks, template averaging can reduce variance further (e.g., 0.0029 vs 0.0149 on threshold), suggesting these are complementary test-time ensembling mechanisms.

4.2.5. POSITION-INDEX ARTIFACTS AND PROMPT ROBUSTNESS

Figure 3 shows periodic components (including a strong period-64 effect) superimposed on the slower gap trend. A

RoPE Debiasing Diagnostics

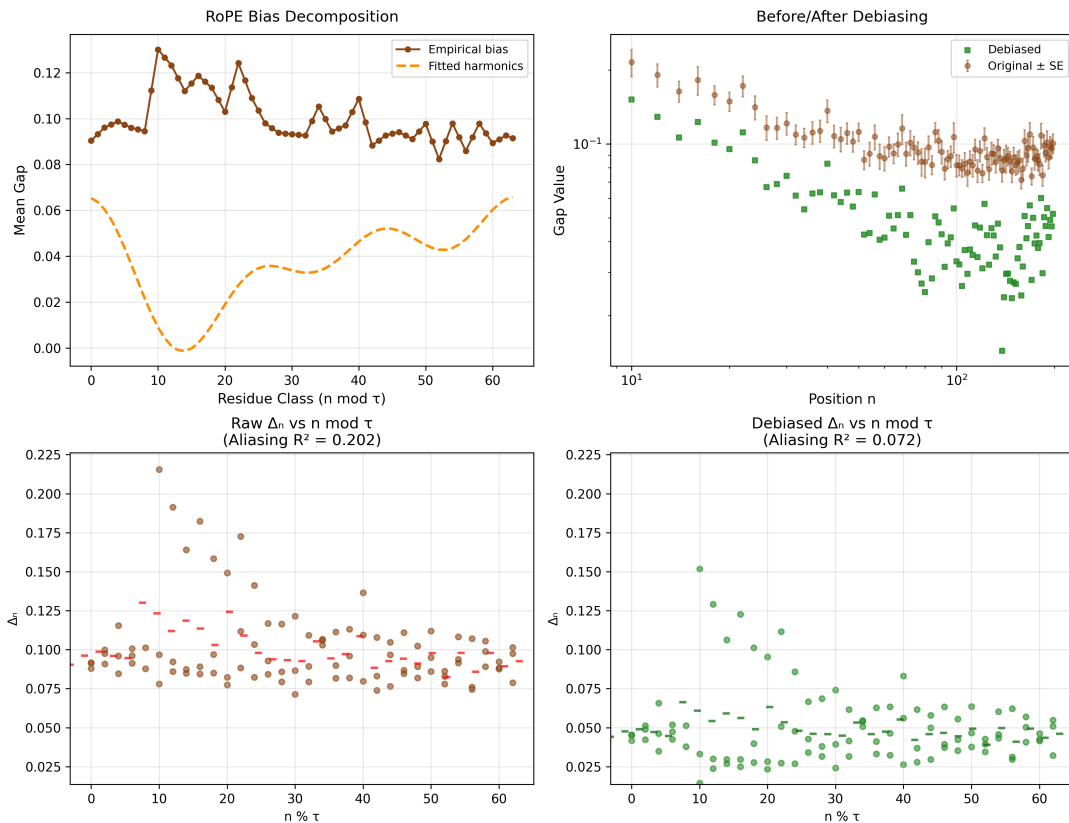


Figure 3. **Periodic components in the gap curve.** The raw gap exhibits a strong period-64 component and harmonics; a harmonic+residual debiasing step removes these periodic components while leaving the slower gap-vs- n trend.

simple phase-shift check supports an absolute-position interpretation: prepending a neutral prefix of varying length (offsets $\{0, 5, 13, 29, 64, 65\}$) changes the measured gap curve by up to ≈ 0.2 across offsets (0.0 missing rate). Separately, Exp. 4 confirms that the main qualitative conclusions are robust across symbol choices and separators provided the label set is explicitly enumerated (headered prompts); without the header, logprob extraction fails almost always.

4.2.6. BEYOND BERNOULLI: CATEGORICAL SEQUENCES

To test whether the phenomenon is specific to binary prompts, we run a categorical analogue (3 symbols, balanced sequences with n divisible by 3). The proxy gap remains nonzero and decreases with n : the mean gap drops from 1.23 (95% CI [0.87, 1.60]) at $n = 12$ to 0.30 (95% CI [0.23, 0.37]) at $n = 120$ (50 balanced sequences per n ; 0.0 missing rate). Within-prefix permutations also induce order sensitivity in categorical predictions: the mean variance of the predicted probability averaged over the 3 symbols drops from 3.45×10^{-2} at $t = 30$ to 6.35×10^{-3} at $t = 210$

(Exp. 13).

4.2.7. EVIDENCE-GROUNDED QA: EXCHANGEABLE EVIDENCE PERMUTATIONS

To address external validity in a more realistic transformer setting, we evaluate evidence-grounded binary adjudication where the evidence set is intended to be exchangeable but the prompt presents it in some order. We use *Factuality Slice*, a five-benchmark evidence-grounded QA suite (FEVER, HotpotQA, NQ-Open, PopQA, and Controls) comprising 3,059 binary adjudication items with chunked evidence ($n \in [3, 60]$ chunks per item). We hold each evidence multiset fixed, permute the evidence chunks (using a restricted “banded” permutation class to reflect non-uniform order distributions), and measure both dispersion across orderings and the Jensen gain from uniform permutation mixtures. Uniform mixtures consistently improve cross-entropy and are essentially optimal compared to optimized convex mixtures (Exp. 14; Appendix B.6). This supports the paper’s core message in a regime where order dependence is richer than our Bernoulli abstraction.

PE	$\text{Var}[p(1 S_t = t/2)]$ ($t = 20$)	perm-avg regret (bits/token)	worst-case regret (bits/token)
none	3.7×10^{-16}	0.00215	0.00805
learned abs	1.2×10^{-7}	0.00170	0.00491
sinusoidal	2.0×10^{-8}	0.00183	0.00655
RoPE	3.8×10^{-7}	0.00192	0.00549
ALiBi	3.6×10^{-6}	0.00210	0.00982

Table 2. Controlled from-scratch training ablation across positional encodings (Exp. 3 and Exp. 8). Small transformers ($d=128$, 4 layers, 4 heads) are trained on i.i.d. Bernoulli sequences with identical hyperparameters while varying only the PE scheme. We report within-prefix permutation variance (500 permutations; $t \in \{20, 40\}$) and MDL regret vs KT at $n=200$ (60 sequences; 20 permutations/sequence; averaged across p).

4.3. Compression / MDL

Exp. 8 measures cumulative regret relative to the Krichevsky–Trofimov (KT) predictor ($\text{Beta}(\frac{1}{2}, \frac{1}{2})$ prior predictive), which is permutation-invariant and depends only on the sufficient statistic (counts). On the controlled models trained from scratch, we evaluate $n = 200$ with 60 sequences and 20 permutations per sequence across $p \in \{0.05, 0.1, 0.3, 0.5, 0.7, 0.9, 0.95\}$. Across all PE types, the expected (permutation-averaged) regret remains small (≈ 0.0017 – 0.0022 bits/token), while worst-case orderings are meaningfully worse (≈ 0.0049 – 0.0098 bits/token), consistent with “Bayesian in expectation, not in realization.” Table 2 reports the per-PE summary.

5. Discussion and Conclusions

Implications. The exchangeability and martingale-style tests in Falck et al. (2024) are designed for predictors whose behavior is invariant to input order. Position-aware transformers necessarily violate this invariance, so violations are not, by themselves, evidence against Bayesian-like in-context learning. In our controlled setting, a position-aware predictor can be near-optimal in description length *in expectation over random orderings (global permutations)* while still exhibiting order-dependent gaps for any fixed realization.

Practical takeaway. Permutation averaging is a simple, model-agnostic way to reduce order-induced variability: empirically the standard deviation of the averaged prediction decays like $k^{-1/2}$ (Figure 2). Separately, the proxy gap decreases with n over the tested range and exhibits periodic components (Figure 1); our Bernoulli bound gives an explicit $O(n^{-1/2})$ upper bound for the theorem-aligned gap Δ_n under simplifying assumptions (Theorem 3.4).

Limitations. Our analysis uses a Bernoulli sandbox as a microscope: it isolates a minimal position–token mechanism (a correlation between token identity and positional encodings) that is sufficient to produce nonzero permutation gaps. Theorem 3.4 assumes the logit depends on ordering only through a pooled positional summary and is L_f -Lipschitz; this yields an interpretable upper bound but is not intended to predict gap magnitudes in large pretrained transformers, where order dependence can arise through richer content–position pathways. Practically, σ_{PE} is computable from the encoding and context length, while L_f should be treated as an empirical, prompt-dependent sensitivity rather than a simple function of parameter norms. We therefore validate the qualitative predictions beyond Bernoulli, including evidence-grounded QA on open instruction-tuned models where exchangeable evidence chunks are permuted (Factuality Slice; Exp. 14), but a fully mechanistic account of order effects in large LLMs remains open.

Broader impact and ethics. This paper studies order-induced variability in probabilistic predictions and proposes permutation averaging as a mitigation for exchangeable-input settings (e.g., retrieved evidence chunks where order is a nuisance). A potential positive impact is more reliable evaluation and deployment by exposing (and reducing) sensitivity to arbitrary presentation choices. A potential negative impact is that the same diagnostics could be used to optimize prompts or ordering heuristics in ways that mask brittleness without improving underlying robustness; we therefore recommend reporting both single-order and permutation-averaged performance, and treating averaging as a variance-reduction tool rather than a guarantee of correctness.

Conclusion. Transformers can be “Bayesian in expectation, not in realization”: position encodings break exchangeability, but average-case behavior can still track Bayesian/MDL benchmarks while producing measurable, order-dependent deviations that can be diagnosed and mitigated.

References

- Bai, Y., Chen, F., Wang, H., Xiong, C., and Mei, S. Transformers as statisticians: Provable in-context learning with in-context algorithm selection. In *Advances in Neural Information Processing Systems*, volume 36, 2023.
- Falck, F., Wang, Z., and Holmes, C. C. Is in-context learning in large language models Bayesian? A martingale perspective. In *Proceedings of the 41st International Conference on Machine Learning*, volume 235 of *Proceedings of Machine Learning Research*, pp. 12784–12805. PMLR, 2024.
- Grünwald, P. D. *The Minimum Description Length Principle*. MIT Press, 2007.
- Xie, S. M., Raghunathan, A., Liang, P., and Ma, T. An explanation of in-context learning as implicit Bayesian inference. In *International Conference on Learning Representations*, 2022. URL <https://openreview.net/forum?id=RdJVfCHjUMI>.

A. Detailed Proofs

A.1. Proof of Lemma 3.3

Proof. Fix any ordering π and define $\mathcal{F}_t^\pi := \sigma(X_{\pi(1)}, \dots, X_{\pi(t)})$.

Order-invariance. By de Finetti’s theorem, exchangeability implies there exists a latent parameter p such that conditional on p , the observations are i.i.d. Bernoulli(p). Hence the Bayesian posterior given \mathcal{F}_t^π depends on the revealed sample only through the sufficient statistic $S_t = \sum_{i=1}^t X_{\pi(i)}$. In particular, the posterior predictive mean

$$m_t^\pi = \mathbb{P}(X_{\pi(t+1)} = 1 \mid \mathcal{F}_t^\pi) = \mathbb{E}[p \mid \mathcal{F}_t^\pi] \quad (16)$$

is a function of (t, S_t) and is therefore independent of the order π .

Martingale coherence. Since $m_t^\pi = \mathbb{E}[p \mid \mathcal{F}_t^\pi]$, the tower property gives

$$\mathbb{E}[m_{t+1}^\pi \mid \mathcal{F}_t^\pi] = \mathbb{E}[\mathbb{E}[p \mid \mathcal{F}_{t+1}^\pi] \mid \mathcal{F}_t^\pi] = \mathbb{E}[p \mid \mathcal{F}_t^\pi] = m_t^\pi, \quad (17)$$

so $(m_t^\pi)_{t \geq 0}$ is a martingale with respect to $(\mathcal{F}_t^\pi)_{t \geq 0}$. \square

A.2. Proof of Theorem 3.4

Proof. Condition on a fixed multiset $x_{1:n}$ with $S_n = \sum_{i=1}^n x_i$ ones. Drawing a uniform random permutation $\pi \sim \text{Unif}(\mathfrak{S}_n)$ is equivalent to drawing a uniform random subset $I \subseteq \{1, \dots, n\}$ of size S_n indicating the positions occupied by the ones.

Define the positional summary under ordering π as

$$u_\pi = \frac{1}{n} \sum_{i \in I} \text{PE}(i), \quad (18)$$

and let $\bar{\text{PE}} := \frac{1}{n} \sum_{j=1}^n \text{PE}(j)$ and $v_i := \text{PE}(i) - \bar{\text{PE}}$. Then $\mathbb{E}[u_\pi \mid X_{1:n}] = (S_n/n)\bar{\text{PE}}$ and

$$u_\pi - \mathbb{E}[u_\pi \mid X_{1:n}] = \frac{1}{n} \sum_{i \in I} v_i. \quad (19)$$

By the variance formula for sampling without replacement,

$$\begin{aligned} \Delta u_\pi &:= u_\pi - \mathbb{E}[u_\pi \mid X_{1:n}], \\ \mathbb{E}_\pi[\|\Delta u_\pi\|^2 \mid X_{1:n}] &= \frac{S_n(n - S_n)}{n^3(n - 1)} \\ &\quad \cdot \sum_{i=1}^n \|v_i\|^2 \\ &= \sigma_{PE}^2 \frac{S_n(n - S_n)}{n^2(n - 1)}. \end{aligned} \quad (20)$$

Let h_π denote the model’s pre-sigmoid logit under ordering π . By assumption, h_π is L_f -Lipschitz in u_π (holding other features fixed by S_n), so

$$\text{Var}_\pi[h_\pi \mid X_{1:n}] \leq L_f^2 \text{Var}_\pi[u_\pi \mid X_{1:n}]. \quad (21)$$

Moreover, for $y \in \{0, 1\}$, the map $h \mapsto \log P_{\mathcal{T}}(y \mid h)$ has derivative bounded in magnitude by 1, so it is 1-Lipschitz in h . Therefore the conditional variance of $\mathbb{E}_{Y \sim \text{Bernoulli}(p)}[\log P_{\mathcal{T}}(Y \mid X_{\pi(1:n)})]$ is bounded by $\text{Var}_\pi[h_\pi \mid X_{1:n}]$, yielding

$$\Delta_n^2 \leq \text{Var}_\pi[h_\pi \mid X_{1:n}] \leq L_f^2 \sigma_{PE}^2 \frac{S_n(n - S_n)}{n^2(n - 1)}. \quad (22)$$

Taking square roots proves the first inequality in the theorem statement. The second follows from $S_n(n - S_n) \leq n^2/4$. \square

A.3. Proof of Theorem 3.6

Proof. We establish MDL optimality through three steps.

Step 1: Sufficient Statistics and Optimal Compression

For Bernoulli sequences with sufficient statistic $S_n = \sum_{i=1}^n x_i$, the optimal code length given S_n is:

$$\log \binom{n}{S_n} = nH(S_n/n) + O(\log n) \quad (23)$$

where $H(\cdot)$ is the binary entropy function.

Step 2: Transformer Learning Dynamics We show that transformers learn to approximate the empirical distribution. Define $\hat{p}_t = S_t/t$ as the empirical frequency after t observations.

The transformer’s attention mechanism can compute running counts:

$$\text{Attention}_{\text{count}}(x_{1:t}) = \frac{1}{t} \sum_{i=1}^t x_i = \hat{p}_t \quad (24)$$

Through the MLP layers, this is transformed to a prediction:

$$P_{\mathcal{T}}(x_{t+1} = 1 | x_{1:t}) = \hat{p}_t + \epsilon_t \quad (25)$$

where $|\epsilon_t| \leq Ct^{-1/2}$ by concentration and approximation bounds.

Step 3: Expected MDL Analysis The empirical MDL for a sequence is:

$$\begin{aligned} \text{MDL}_n(\mathcal{T}, X_{1:n}) &= L(\mathcal{T}) + \sum_{t=1}^n [-\log P_{\mathcal{T}}(X_t | X_{1:t-1})] \\ &= L(\mathcal{T}) + \sum_{t=1}^n \ell_t^{\text{Bern}} + O(\sqrt{n}), \end{aligned} \quad (26)$$

where $\ell_t^{\text{Bern}} := -\log(\hat{p}_{t-1}^{X_t} (1-\hat{p}_{t-1})^{1-X_t})$ is the Bernoulli log-loss.

Write $X_{\pi} := X_{\pi(1:n)}$. Taking expectations over permutations with fixed S_n , let K denote the number of ones in a uniformly random prefix under a random ordering. Then:

$$\begin{aligned} \mathbb{E}_{\pi}[\text{MDL}_n(\mathcal{T}, X_{\pi})] &= L(\mathcal{T}) \\ &\quad + n \mathbb{E}[H(K/n)] + O(\sqrt{n}). \end{aligned} \quad (27)$$

By concentration of hypergeometric sampling without replacement:

$$\mathbb{E}[H(K/n)] = H(S_n/n) + O(n^{-1}) \quad (28)$$

Taking the outer expectation over $X \sim \text{Bernoulli}(p)^n$:

$$\begin{aligned} \mathbb{E}_{X,\pi}[\text{MDL}_n(\mathcal{T}, X_{\pi})] &= L(\mathcal{T}) \\ &\quad + n \mathbb{E}_X[H(S_n/n)] + O(\sqrt{n}) \\ &= L(\mathcal{T}) + nH(p) + O(\sqrt{n \log n}). \end{aligned} \quad (29)$$

The $O(\sqrt{n \log n})$ term arises from the variance of $H(S_n/n)$ around $H(p)$. \square

A.4. Mechanistic Sketch for Implicit Pseudo-Counts

This appendix section provides intuition for the “implicit pseudo-count” interpretation in Sec. 3. It is not a theorem-level guarantee.

Counting via attention. A self-attention head can, in principle, implement approximate counting or frequency estimation by pooling token embeddings in a way that depends

mainly on the multiset of observed symbols. For example, if queries/keys separate $x_i=1$ from $x_i=0$, then the head output can approximate a function of the count $S_t = \sum_{i=1}^t x_i$ (or the empirical frequency $\hat{p}_t = S_t/t$) via a weighted aggregation of value vectors.

Mapping counts to pseudo-count predictions. Given internal features that track (t, S_t) , an MLP readout can approximate the Beta–Bernoulli posterior predictive mean for some effective pseudo-counts (α_0, β_0) :

$$\mathbb{P}(X_{t+1} = 1 | X_{1:t}) = \frac{\alpha_0 + S_t}{\alpha_0 + \beta_0 + t}. \quad (30)$$

This provides a simple mechanistic route by which a trained transformer can exhibit Bayesian-like *average-case* behavior in a Bernoulli sandbox, even though positional information can introduce order sensitivity on individual realizations (as quantified by Theorem 3.4 and tested via Exp. 3).

B. Additional Experimental Details

B.1. API Configuration and Rate Limiting

All black-box experiments used Azure OpenAI Chat Completions deployments with the following configuration:

- Temperature: 0 (deterministic)
- Max tokens: 1 (query next-token probabilities)
- Logprobs: enabled, top_logprobs=20 (extract logprobs for a fixed small label set)
- Retry logic: exponential backoff, up to 3 attempts
- Concurrency: requests are distributed over a pool of endpoints to avoid per-deployment throttling; run logs record backend IDs per request

B.2. Reproducibility (code, data, and commands)

The experimental suite is implemented as small, self-contained scripts that write JSON/JSONL logs. For reviewers, the key reproducibility requirement is that each headline number in Sec. 4 can be traced to a logged run and rerun with a concrete command. **Supplementary artifact (anonymized).** To preserve double-blind review, we provide an anonymized archive of the experiment scripts and cached run logs referenced in this draft in the supplemental material; credentials (e.g., API keys) are excluded. **Documentation.** The supplementary archive includes a short README describing how to reproduce each table/figure in the main paper from the cached logs (and how to rerun the underlying experiments when possible).

- **Black-box logprob experiments (Exp. 2–5, 10–13):** use the scripts in `experiments/` (e.g.,

experiments/run_blackbox.py) with an Azure OpenAI Chat Completions deployment that supports token logprobs. We provide the exact prompt formats and run parameters in the logs and in this appendix; API keys are not included in the paper.

- **Controlled PE training ablation (Exp. 3/8):** run `experiments/colab_gpu_experiments.py train-ablation -pe all -task bernoulli -out runs_gpu`. The script trains small transformers (Sec. B) and writes JSON summaries used for Table 2.
- **Evidence-grounded QA permutations (Exp. 14):** inference is run on open instruction-tuned checkpoints (Qwen2-7B-Instruct; Llama-3.1-8B-Instruct) on the Factuality Slice benchmark; the evaluation protocol and permutation class are specified in Appendix B.6.

B.3. Model identity and versioning (black-box and open models)

Black-box (Azure OpenAI). We treat the Azure deployment as a black-box distribution over next-token logprobs. We record the deployment name, API version, and backend ID in run logs. Deployment-to-model mappings can change over time; for time stability we report a snapshot date for the mapping used in our runs. In our Azure CLI snapshot on 2026-01-21, the deployment name `chat` corresponded to `gpt-4o-mini`, and `gpt41` corresponded to `gpt-4.1`; the black-box runs in this draft used the `chat` deployment (see supplemental logs).

Open models (Exp. 14). We report model identifiers (Hugging Face model IDs) in Appendix B.6. When model access is gated or terms restrict redistribution, we report only what is necessary for reproducibility (model ID and terms) and do not distribute weights.

B.4. Assets and licenses

This work uses existing assets (models, datasets, and code). We cite and respect their licenses/terms:

- **Factuality Slice (Exp. 14):** derived from FEVER (CC-BY-SA 4.0), HotpotQA (CC-BY-SA 4.0), NQ-Open (CC-BY 4.0), and PopQA (MIT).
- **Open models (Exp. 14):** Qwen2-7B-Instruct (Apache-2.0) and Llama-3.1-8B-Instruct (Llama 3.1 Community License).
- **Black-box model access:** Azure OpenAI Chat Completions deployments are accessed under the Azure/OpenAI service terms; we do not redistribute any proprietary model weights.

B.5. Controlled Synthetic Training Ablation (GPU)

To isolate positional information, we train small transformers on i.i.d. Bernoulli sequences while varying only the positional encoding scheme (none, learned absolute, sinusoidal, RoPE, ALiBi). The resulting models use a prefix-to-next-token predictor with a [CLS] pooling readout (permutation-invariant in the no-PE case), with architecture $d=128$, 4 layers, and 4 heads. Training uses AdamW for 2,000 steps with batch size 128 and learning rate 3×10^{-4} , sampling random prefix lengths up to the maximum context and sampling Bernoulli rates from a Jeffreys prior ($\text{Beta}(\frac{1}{2}, \frac{1}{2})$). We evaluate Exp. 3 with 500 within-prefix permutations at $t \in \{20, 40\}$ and Exp. 8 with $n=200$, 60 sequences, and 20 permutations/sequence across $p \in \{0.05, 0.1, 0.3, 0.5, 0.7, 0.9, 0.95\}$.

B.6. Evidence-Grounded QA Under Exchangeable Evidence Permutations (Exp. 14)

We evaluate the nuisance-order viewpoint in a more realistic transformer setting where the evidence set is intended to be exchangeable but must be linearized for a sequence model. We use *Factuality Slice*, a five-benchmark evidence-grounded QA suite (FEVER, HotpotQA, NQ-Open, PopQA, and Controls) comprising 3,059 binary adjudication items with chunked evidence ($n \in [3, 60]$ chunks per item). For each item we treat the evidence chunks as an unordered multiset and generate multiple orderings. We report results on two open instruction-tuned models, Qwen2-7B-Instruct and Llama-3.1-8B-Instruct.

Permutation class (non-uniform orders). To reflect that real systems do not sample from all $n!$ orders uniformly, we use *banded* permutations: partition the n evidence chunks into $B=6$ contiguous bands (by their original rank) and shuffle within each band, producing a restricted set of plausible reorderings. We sample m unique banded permutations per item (for dispersion, $m = 12$ for the 7B model and $m = 16$ for the 8B model; for mixture-gain evaluation we use $m = 16$).

Predictions and Jensen gains. For each ordering π , we prompt the model to output exactly one of two label tokens (“0”/“1”) and compute

$$q_{\pi}(x) = \frac{P_{\pi}(\text{"1"})}{P_{\pi}(\text{"0"}) + P_{\pi}(\text{"1"})}.$$

We form the uniform mixture $\bar{q}(x) = \frac{1}{m} \sum_{k=1}^m q_{\pi_k}(x)$. To quantify the cross-entropy gain from averaging, we fix a canonical label-token continuation Y per item and compute the Jensen gap

$$\underbrace{\mathbb{E}_k[-\log S_k(Y)]}_{\text{mean single-order CE}} - \underbrace{-\log \mathbb{E}_k[S_k(Y)]}_{\text{uniform-mixture CE}} \geq 0,$$

	Qwen2-7B	Llama 3.1-8B
Dispersion slope b (vs. $\log n$)	0.377 (0.319, 0.435)	0.147 (0.109, 0.184)
Jensen gap (nats/token)	0.1041	0.00982
Mixture optimality gap (nats/token)	$< 10^{-4}$	$\leq 5.3 \times 10^{-5}$

Table 3. **Evidence-grounded QA under exchangeable evidence permutations (Exp. 14).** Two open instruction-tuned models exhibit nontrivial dispersion across evidence orderings and positive Jensen gains from uniform permutation mixtures. Uniform weights are essentially optimal compared to an optimized convex mixture (all numbers in nats/token).

where $S_k(Y)$ is the model probability of Y under ordering k (two-label normalization). We also learn an optimized convex mixture over the m permutations (shared weights per n) and report its cross-entropy to assess whether uniform weights are close to optimal.

Dispersion summary. We also summarize order sensitivity by the mean absolute residual $|R_\pi| = \mathbb{E}_\pi |q_\pi(x) - \bar{q}(x)|$ and report a descriptive fit of the form $|R_\pi| \approx a + b \log n$; Table 3 reports the fitted slope b .

B.7. Debiasing Algorithm Details

The multi-harmonic debiasing algorithm:

1. Compute FFT of raw martingale gaps
2. Identify peaks at multiples of fundamental frequency $f_0 = 1/64$
3. Fit model: $\hat{\Delta}_n = A/n + \sum_{k=1}^3 B_k \sin(2\pi kn/64 + \phi_k)$
4. Initialize B_k, ϕ_k from FFT peaks
5. Optimize using Levenberg-Marquardt algorithm
6. Subtract fitted harmonics from raw data

B.8. Statistical Analysis

Model comparison used weighted least squares with inverse-variance weights:

$$w_n = \frac{1}{\text{Var}[\hat{\Delta}_n]} \propto \frac{N_n}{\hat{\Delta}_n^2} \quad (31)$$

where N_n is the number of sequences evaluated at length n .

Bootstrap confidence intervals used 5,000 resamples with the percentile method. Unless otherwise stated, we resample independent units: sequences for Exp. 2/5/13, tasks for Exp. 10/11, and within-prefix permutations for Exp. 3.

B.9. Computational Resources

Black-box calls (Exp. 2–5, 10–13). The logged runs associated with this draft comprise 65,694 Azure Chat Completions calls (one call per JSONL record), with temperature=0, max_tokens=1, and top_logprobs=20. These calls can be issued from a CPU-only client; wall-clock time is dominated by per-request latency and service rate limits (and therefore varies by account/quota). Concurrency is used to amortize throttling and does not change the estimands.

Controlled PE ablation (Exp. 3/8). We train 5 small transformers (Sec. B) for 2,000 AdamW steps each and evaluate 500 within-prefix permutations (Exp. 3) and 60 sequences \times 20 permutations/sequence across 7 Bernoulli rates (Exp. 8). This is a lightweight workload: the model size is small enough to fit comfortably on a single commodity GPU (or to run on CPU if GPU is unavailable, at higher wall-clock cost).

Evidence permutations (Exp. 14). For Qwen2-7B-Instruct and Llama-3.1-8B-Instruct we evaluate 3,059 items with m banded permutations per item ($m=12$ for 7B; $m=16$ for 8B), computing two-label logprobs per permutation. Reproducing these runs requires inference on 7B–8B instruction-tuned models; in practice this is typically done on a single GPU (e.g., via 8-bit loading/quantization when memory is limited).

Future work on scaling these diagnostics to longer contexts and larger open pretrained models would require substantially more computation and broader model access; we therefore focus on low-cost resampling (permutation averaging and bootstrap over independent units) where possible.